Integral based Curvature Estimators in Digital Geometry

David Coeurjolly, Jacques-Olivier Lachaud, Jérémy Levallois

Integral based Curvature Estimators in Digital Geometry[⋆]

David Coeurjolly[1], Jacques-Olivier Lachaud[2], and Jérémy Levallois[1,2]

[1] Université de Lyon, CNRS
INSA-Lyon, LIRIS, UMR5205, F-69621, France
[2] Université de Savoie, CNRS
LAMA, UMR5127, F-73776, France

Abstract. In many geometry processing applications, the estimation of differential geometric quantities such as curvature or normal vector field is an essential step. In this paper, we investigate a new class of estimators on digital shape boundaries based on Integral Invariants. More precisely, we provide both proofs of multigrid convergence of curvature estimators and a complete experimental evaluation of their performances.

Keywords: Digital geometry, curvature estimation, multigrid convergence, integral invariants

1 Introduction

In many shape processing applications, differential quantities estimation on the shape boundary is usually an important tool. When evaluating a differential estimator on discrete or digital data, we need a way to mathematically link the estimated quantity to the expect Euclidean one. In Digital Geometry, we usually consider multigrid convergence principles: when the shape is digitized on a grid with resolution tending to zero, the estimated quantity should converge to the expected one [4]. Hence, in dimension 2, parameter free convergence results have been obtained for length [3] and normal vector estimation [20]. Based either on binomial convolution principles [15, 5], or polynomial fitting [18], convergence results can also be obtained for higher order derivatives of digital curves. Algorithms are parametrized by the size of the convolution or fitting kernel support and convergence theorem holds when such support size is an increasing function of the grid resolution and some shape characteristics. For curvature estimation along 2D curves, multigrid convergence of parameter free estimator is still challenging, although accurate experimental results have been obtained [19]. In 3D, several empirical methods exist for estimating curvatures, but none achieves multigrid convergence (e.g. see [6]).

In geometry processing, interesting mathematical tools have been developed to design differential estimators on smooth surfaces based on integral invariants

[⋆] This work has been mainly funded by DigitalSnow ANR-11-BS02-009 research grants

[17, 16]. They consist in moving a kernel along the shape surface and in computing integrals on the intersection between the shape and the kernel. Authors have demonstrated that some integral quantities provide interesting curvature information when the kernel size tends to zero.

The contributions of the paper can be sketched as follows. First, we define digital versions of integral invariant estimators for which convergence results can be obtained when the grid resolution tends to zero. We provide an explicit formula for the kernel size, which guarantees uniform convergence for smooth enough curves (Sect. 3). Furthermore, we demonstrate that these estimators have efficient implementations and that they compete with classical ones in terms of accuracy (Sect. 4). We also illustrate the strength of the framework to design mean and Gaussian curvature estimators on surfaces in $\mathbb{Z}^3$.

2 Preliminaries

2.1 Shapes, digital shapes and multigrid convergence

Since we are interested in evaluating both theoretically and experimentally the behavior of a given differential estimator on digital object boundaries, we first have to formalize links between Euclidean objects and digital ones with the help of a digitization process. Let us consider a family $\mathbb{X}$ of smooth and compact subsets of $\mathbb{R}^d$. In Section 3 we will be more precise on the notion of smoothness for shapes $X \in \mathbb{X}$. We denote $\mathtt{D}_h(X)$ the digitization of X in a $d-$dimensional grid of resolution h. More precisely, we consider classical Gauss digitization defined as

$$\mathtt{D}_h(X) \overset{def}{=} \left(\frac{1}{h} \cdot X \right) \cap \mathbb{Z}^d \qquad (1)$$

where $\frac{1}{h} \cdot X$ is the uniform scaling of X by factor $\frac{1}{h}$. Furthermore, the set ∂X denotes the frontier of X (i.e. its topological boundary). If $z \in \mathbb{Z}^d$, then Q_z denotes the unit d-dimensional cube of $\mathbb{R}^d$ centered on z. The *h-frontier $\Delta_h Z$ of a digital set $Z \subset \mathbb{Z}^d$* is defined as $\Delta_h Z \overset{def}{=} \partial(h \cdot \cup_{z \in Z} Q_z)$. Therefore, the h-frontier of $\mathtt{D}_h(X)$ is a $d-1$-dimensional subset of $\mathbb{R}^d$, which is close to ∂X. We will precise the term "close" later in this subsection. Since this paper deals with multigrid convergence, digital shapes will always come from the digitization of continuous shapes. To simplify notations, the h-frontier of the Gauss digitization at step h of a shape X will simply be denoted by $\partial_h X \overset{def}{=} \Delta_h \mathtt{D}_h(X)$, and called later on *$h$-boundary of X*.

As discussed in various previous works, the idea of multigrid convergence is that when we define a quantity estimator on $\mathtt{D}_h(X)$, we check if the estimated quantity converges (theoretically and/or experimentally) to the associated one on X when h tends to zero. In this paper, we focus on local and global estimated quantities. More formally,

Definition 1 (Multigrid convergence for local geometric quantities). *A local discrete geometric estimator $\hat{E}$ of some geometric quantity E is* multigrid convergent *for the family* $\mathbb{X}$ *if and only if, for any* $X \in \mathbb{X}$*, there exists a grid step* $h_X > 0$ *such that the estimate* $\hat{E}(\mathtt{D}_h(X), \hat{x}, h)$ *is defined for all* $\hat{x} \in \partial_h X$ *with* $0 < h < h_X$*, and for any* $x \in \partial X$*,*

$$\forall \hat{x} \in \partial_h X \text{ with } \|\hat{x} - x\|_\infty \leq h, |\hat{E}(\mathtt{D}_h(X), \hat{x}, h) - E(X, x)| \leq \tau_{X,x}(h), \tag{2}$$

where $\tau_{X,x} : \mathbb{R}^+ \setminus \{0\} \to \mathbb{R}^+$ *has null limit at* 0*. This function defines the speed of convergence of* $\hat{E}$ *toward* E *at point* x *of* X*. The convergence is* uniform *for* X *when every* $\tau_{X,x}$ *is bounded from above by a function* τ_X *independent of* $x \in \partial X$ *with null limit at* 0*.*

When a geometrical quantity is gobal (*e.g.* area or volume), we do not need explicit mapping between ∂X and $\partial_h X$, and Def 1 can be rephrased to define *multigrid convergence of global geometric quantities* [4]. A local discrete estimator thus estimates a geometric quantity at points on the h-frontier of a digital set, otherwise said at any point on the interpixel representation of the digital set boundary. This definition encompasses usual definitions where input points are pointels, linels or surfels. In some proofs, a more precise mapping between points $x \in \partial X$ and $\hat{x} \in \partial_h X$ is required. For a $2D$ shape X with bounded curvature $\kappa_{\max}$ along its boundary, this mapping is the *back-projection* map (cf Fig. 1-($right$)). Let $n(X, x, l)$ be the straight segment, centered on x, aligned with the normal vector at x along ∂X, and of half-length l.

Definition 2 (Back-projection π_h^X [12]). *For* $0 < h \leq 1/\kappa_{\max}$*, let* $\pi_h^X : \partial_h X \to \partial X, \hat{x} \mapsto x = \pi_h^X(\hat{x})$*, where* x *is the only point such that* $\hat{x} \in n(X, x, \frac{\sqrt{2}}{2} h)$*.*

Lemma B.9 [12] indicates that the map π_h^X is well-defined and onto. Lemma B.10 further tells that this map is continuous. It shows that the boundaries $\partial_h X$ and ∂X are indeed close, since their Hausdorff distance is no greater than $\frac{\sqrt{2}}{2} h$.

2.2 Integral invariants theory

In Geometry Processing, integral invariants have been widely investigated to construct estimators of differential quantities (see [17, 16] for a complete overview). For short, the main idea is to move a kernel on points $x \in \partial X$ and to compute integrals on the intersection between X and the kernel. Even if different kernels (Euclidean ball, Euclidean sphere,...) and different integration functions can be considered, we focus here on volumetric integral invariants defined as follows:

Definition 3. *Given* $X \in \mathbb{X}$ *and a radius* $r \in \mathbb{R}^{+*}$*, the volumetric integral* $V_r(x)$ *at* $x \in \partial X$ *is given by (see Fig. 1–($left$))*

$$V_r(x) \stackrel{def}{=} \int_{B_r(x)} \chi(p) dp \,, \tag{3}$$

where $B_r(x)$ *is the Euclidean ball with radius* r *and center* x *and* $\chi(p)$ *the characteristic function of* X*. In dimension 2, we simply denote* $A_r(x)$ *such quantity.*

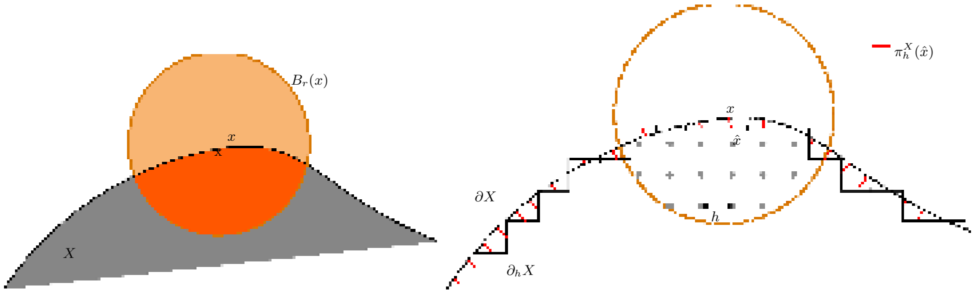

Fig. 1. Integral invariant computation (*left*) and notations (*right*) in dimension 2.

Several authors have detailed connections between $V_r(x)$ and curvature (resp. mean curvature) at x for shapes in $\mathbb{R}^2$ (resp. $\mathbb{R}^3$) [2, 17, 16].

Lemma 1 ([16]). *For a sufficiently smooth shape X in $\mathbb{R}^2$ $x \in \partial X$, we have*

$$A_r(x) = \frac{\pi}{2}r^2 - \frac{\kappa(X,x)}{3}r^3 + O(r^4) \tag{4}$$

where $\kappa(X,x)$ is the curvature of ∂X at x. For a sufficiently smooth shape X in $\mathbb{R}^3$ and $x \in \partial X$, we have

$$V_r(x) = \frac{2\pi}{3}r^3 - \frac{\pi H(X,x)}{4}r^4 + O(r^5) \tag{5}$$

where $H(X,x)$ is the mean curvature of ∂X at x.

Such results are obtained by Taylor expansion at x of the surface ∂X approximated by a parametric function $y = f(x)$ in 2D and $z = f(x,y)$ in 3D. From Eq. (4) and (5) and with a fixed radius r, one can derive local estimators $\tilde{\kappa}_r(x)$ and $\tilde{H}_r(x)$ respectively:

$$\tilde{\kappa}_r(X,x) \overset{def}{=} \frac{3\pi}{2r} - \frac{3A_r(x)}{r^3}, \quad \tilde{H}_r(X,x) \overset{def}{=} \frac{8}{3r} - \frac{4V_r(x)}{\pi r^4} \tag{6}$$

In this way, when r tends to zero, both estimated values will converge to expected ones (respectively κ and H). More formally:

$$\tilde{\kappa}_r(X,x) = \kappa(X,x) + O(r), \quad \tilde{H}_r(X,x) = H(X,x) + O(r) \tag{7}$$

We mention additional results which allows us to access to directional information such as principal curvature directions. Instead of computing the measure of $B_r(x) \cap X$ as in Def. 3, we consider its covariance matrix. In [17], authors have demonstrated that eigenvalues and eigenvectors of the covariance matrix provide principal curvature and principal direction information. We do not detail this approach here but we give preliminary results on digital curvature estimators based on this fact in Sect. 4.

When dealing with digital shapes $\mathtt{D}_h(X)$, implementation of these estimators becomes straightforward: choose a radius r, center an Euclidean (or digital) ball at chosen points of $\partial_h X$ (e.g. centroids of linels or surfels), compute the intersection in terms of number of pixels/voxels and finally estimate $\tilde{\kappa}$ and $\tilde{H}$ using (6). However, several issues are hidden is this approach: What are meaningful values for r according to the shape size and geometry ? Do points of $\partial_h X$ converge to points $x \in \partial X$ for which Lemma 1 is valid ? Does counting the number of pixels (resp. voxels) converge to $A_r(x)$ (resp. $V_r(x)$) ? The rest of the paper addresses all these questions.

3 Multigrid convergence of curvature estimator in digital space

We first recall multigrid convergence theorems for area and volume estimation by counting which will be useful to design digital version of integral invariants. A new digital curvature estimator $\hat{\kappa}_r$ is then defined (Eq. (11)) and its multigrid convergent properties are established (Theorems 1 and 2).

3.1 Area or volume estimation by counting

Area in the plane and volume in the space can be estimated by counting the number of digital points belonging to the shape. Given digital shapes $Z \subset \mathbb{Z}^2$ and $Z' \subset \mathbb{Z}^3$, the *discrete area and volume estimators by counting at step h* are defined as $\widehat{\mathrm{Area}}(Z, h) \overset{def}{=} h^2 \mathrm{Card}(Z)$ and $\widehat{\mathrm{Vol}}(Z', h) \overset{def}{=} h^3 \mathrm{Card}(Z')$. Now, if those digital shapes Z and Z' come from digitizations of Euclidean shapes X and X', then as the digitization step h gets finer, these estimators give better and better estimation of the area of X and of the volume of X' respectively. We have the following convergence results, letting X be a finite convex shape of $\mathbb{R}^2$ and X' defined similarly in $\mathbb{R}^3$:

$$\widehat{\mathrm{Area}}(\mathtt{D}_h(X), h) = \mathrm{Area}(X) + O(h^\beta), \quad \widehat{\mathrm{Vol}}(\mathtt{D}_h(X'), h) = \mathrm{Vol}(X') + O(h^\gamma), \quad (8)$$

where $\beta = 1$ in the general case (known since Gauss and Dirichlet according to [10]) and may be improved to $\frac{15}{11} - \epsilon$, $\epsilon > 0$ arbitrary small, when the shape boundary is C^3 with non-zero curvature [8]. Similar results hold in 3D, $\gamma = 1$ is the general case (e.g. see [11]) while $\gamma = \frac{243}{158}$ for smoother boundary [7]. In fact, preceding equations hold whenever the shape boundary can be decomposed in a finite number of convex pieces [9].

3.2 Estimation of integral invariants

We are mainly concerned by the estimation of the quantity $A_r(x) = \mathrm{Area}(B_r(x) \cap X)$ of Def. 3 at a step h. We cannot readily use Eq. (8) to estimate this area: in this case, the big “O” notation hides the fact that the involved constant depend on the shape size, scale and maximal curvature. It is obvious that doubling the size of X will induce a better estimate of the area of $2 \cdot X$ at the same scale h. This is a problem with integral invariants, since the involved balls have a radius r which tends toward 0 as h tends toward 0. We need to normalize our area estimation so that the error is no more influenced by the scale. Hence we estimate the area $A_r(x)$ as follows:

$$\begin{aligned}
\widehat{\mathrm{Area}}(\mathtt{D}_h(B_r(x)\cap X),h) &\overset{def}{=} h^2\mathrm{Card}((\frac{1}{h}\cdot(B_r(x)\cap X))\cap\mathbb{Z}^2),\\
&= h^2\mathrm{Card}((\frac{r}{h}\cdot(B_1(\frac{1}{r}\cdot x)\cap\frac{1}{r}\cdot X))\cap\mathbb{Z}^2),\\
&= r^2\frac{h^2}{r^2}\mathrm{Card}((\frac{r}{h}\cdot(B_1(\frac{1}{r}\cdot x)\cap\frac{1}{r}\cdot X))\cap\mathbb{Z}^2),\\
&= r^2\widehat{\mathrm{Area}}(\mathtt{D}_{h/r}(B_1(\frac{1}{r}\cdot x)\cap\frac{1}{r}\cdot X),h/r),
\end{aligned}$$

by definitions of $\widehat{\mathrm{Area}}$ and $\mathtt{D}$. We insert (8) in the right handside term:

$$\widehat{\mathrm{Area}}(\mathtt{D}_h(B_r(x)\cap X),h) = r^2\left(\mathrm{Area}(B_1(\frac{1}{r}\cdot x)\cap\frac{1}{r}\cdot X)+O((h/r)^\beta)\right). \tag{9}$$

Let $SB(r)$ denotes the set $B_1(\frac{1}{r}\cdot x)\cap\frac{1}{r}\cdot X$. The constant K_1 associated to the big "O" depends only of the maximal curvature of $\partial SB(r)$. The curvature is not defined on the subset $\partial B_1(\frac{1}{r}\cdot x)\cap\frac{1}{r}\cdot\partial X$, but its influence on the area estimation is negligible (at most $O(h^2)$). The remaining part of $\partial SB(r)$ has a maximal curvature which is obviously 1 for sufficiently small r. Indeed, since X has bounded curvature, its dilated $\frac{1}{r}\cdot\partial X$ becomes flat at point $\frac{1}{r}\cdot x$, the maximal curvature value 1 is thus induced by $\partial B_1(x)$. We conclude that there exists some r_0 such that the constant K_1 holds for arbitrary $r<r_0$. Developping the big "O" with K_1 and inserting in (9) the straightforward relation $A_r(x) = \mathrm{Area}(B_r(x)\cap X) = r^2\mathrm{Area}(B_1(\frac{1}{r}\cdot x)\cap\frac{1}{r}\cdot X)$, we finally obtain:

$$|\widehat{\mathrm{Area}}(\mathtt{D}_h(B_r(x)\cap X),h) - A_r(x)| \leq K_1 h^\beta r^{2-\beta}. \tag{10}$$

The preceding convergence relation holds for $h\leq r\leq r_0$, and is also valid when x is any point of $\mathbb{R}^2$, not necessarily a point of ∂X. Note that the constant K_1 is independent of the shape X (but not r_0).

The same reasoning is valid in 3D: The curvature is then not defined on the subset $\partial B_1(\frac{1}{r}\cdot x)\cap\frac{1}{r}\cdot\partial X$, which tends toward the unit circle as $r\to 0$. The induced error on volume estimation is then the number of intersected voxels ($\approx 2\pi/h$) times the volume of a voxel (h^3), and is hence negligible. Maximal curvatures are obviously 1 for sufficiently small r. The same relation as (10) holds for $\widehat{\mathrm{Vol}}$, where β is replaced by γ.

3.3 Digital curvature estimator

In a similar spirit to (6), we define the *integral digital curvature estimator* $\hat{\kappa}_r$ of a digital shape Z at point $x\in\mathbb{R}^2$ and step h as:

$$\forall 0<h<r, \hat{\kappa}_r(Z,x,h) \overset{def}{=} \frac{3\pi}{2r} - \frac{3\widehat{\mathrm{Area}}(B_{r/h}(\frac{1}{h}\cdot x)\cap Z,h)}{r^3}. \tag{11}$$

To establish its multigrid convergence when Z is the digitization of some subset X of $\mathbb{R}^2$, we proceed in two phases, depending on whether or not we know the exact position of point x on ∂X or only an approximation $\hat{x}$ on $\partial_h X$.

Convergence when $\boldsymbol{x \in \partial X}$. Using relations on integral invariants (6), (10), and relation $\mathtt{D}_h(B_r(x) \cap X) = B_{r/h}(\frac{1}{h} \cdot x) \cap \mathtt{D}_h(X)$, we obtain for $r < r_0$:

$$|\hat{\kappa}_r(\mathtt{D}_h(X), x, h) - \kappa(X, x)| = \left| \frac{3\pi}{2r} - \frac{3\widehat{\mathrm{Area}}(B_{r/h}(\frac{1}{h} \cdot x) \cap \mathtt{D}_h(X), h)}{r^3} - \kappa(X, x) \right|,$$

$$\begin{aligned}
|\hat{\kappa}_r(\mathtt{D}_h(X), x, h) - \kappa(X, x)| &\leq \left| \frac{3\pi}{2r} - \frac{3\mathrm{Area}(B_r(x) \cap X)}{r^3} - \kappa(X, x) \right| + 3K_1 \frac{h^\beta}{r^{1+\beta}} \\
&\leq |\tilde{\kappa}_r(X, x) - \kappa(X, x)| + 3K_1 \frac{h^\beta}{r^{1+\beta}}, \\
&\leq O(r) + 3K_1 \frac{h^\beta}{r^{1+\beta}}, \quad \text{(using Eq. (7))}. \qquad (12)
\end{aligned}$$

There are two error terms, both of which depends on the choice of the ball radius r. We propose to set $r = kh^\alpha$, and to choose k and α so as to minimize the error bound. Denoting by K_2 the constant in the big "O", we derive:

$$|\hat{\kappa}_r(\mathtt{D}_h(X), x, h) - \kappa(X, x)| \leq K_2 k h^\alpha + \frac{3K_1}{k^{1+\beta}} h^{\beta - \alpha(1+\beta)}. \qquad (13)$$

Since one error term in (13) increases with α while the other decreases with α, the minimum is achieved when the exponents are the same (solve $\alpha = \beta - \alpha(1+\beta)$). The constant k is then obtained by studying its variation at the optimal α. We obtain the convergence theorem below.

Theorem 1 (Convergence of digital curvature estimator $\hat{\kappa}_r$ along ∂X). *Let X be some convex shape of $\mathbb{R}^2$, with at least C^2-boundary and bounded curvature. Then $\exists h_0, K_1, K_2$, such that*

$$\forall h < h_0, r = k_m h^{\alpha_m}, |\hat{\kappa}_r(\mathtt{D}_h(X), x, h) - \kappa(X, x)| \leq K h^{\alpha_m}, \qquad (14)$$

where $\alpha_m = \frac{\beta}{2+\beta}$, $k_m = ((1+\beta)K_1/K_2)^{\frac{1}{2+\beta}}$, $K = K_2 k_m + 3K_1/k_m^{1+\beta}$. When the boundary of X is C^3 without null curvature points, the exponent $\alpha_m = \frac{15}{37} - \epsilon \approx 0.405$, otherwise $\alpha_m = \frac{1}{3}$.

Convergence for $\boldsymbol{\hat{x} \in \partial_h X}$. Unfortunately, the exact position of x is unknown in digital geometry applications. We only know some digital point $\hat{x} \in \partial_h X$, which is close to some point $x \in \partial X$. More precisely, the back-projection is used to determine x as $\pi_h^X(\hat{x})$. Integral invariants are not directly applicable since estimator $\hat{\kappa}_r$ at $\hat{x}$ is then related to $A_r(\hat{x})$, where $\hat{x}$ does not generally lie onto ∂X. We have to determine the error between the area measure at $\hat{x}$ and at x.

Notice first that point $\hat{x}$ lies on the normal direction to ∂X at x, at a distance $\delta \overset{def}{=} \|x-\hat{x}\|_2$. In 3D, we could use Theorem 7 of [17]. In 2D, we achieve similarly:

$$|A_r(\hat{x}) - A_r(x)| = 2r\delta(1 + O(r^2) + O(\delta)). \tag{15}$$

We write (10) at point $\hat{x}$ (recall that $A_r(y) = B_r(y) \cap X$) and insert (15):

$$\begin{aligned} &|\widehat{\text{Area}}(\mathtt{D}_h(B_r(\hat{x}) \cap X), h) - A_r(\hat{x})| \le K_1 h^\beta r^{2-\beta}, \quad \text{which implies} \\ &|\widehat{\text{Area}}(\mathtt{D}_h(B_r(\hat{x}) \cap X), h) - A_r(x)| \le K_1 h^\beta r^{2-\beta} + 2r\delta(1 + O(r^2) + O(\delta)). \end{aligned} \tag{16}$$

In order to get the curvature estimator, we follow the same reasoning as in (12) but we use (16) instead of (10), which gives:

$$|\hat{\kappa}_r(\mathtt{D}_h(X), \hat{x}, h) - \kappa(X, x)| \le O(r) + 3K_1 \frac{h^\beta}{r^{1+\beta}} + \frac{6\delta}{r^2}(1 + O(r^2) + O(\delta)). \tag{17}$$

We know that $\delta \le \frac{\sqrt{2}}{2}h$ (see above). In fact, in some cases (see [13]), we can hope to get a better localization of x wrt $\hat{x}$. Therefore we write $\delta = O(h^{\alpha'})$, where $\alpha' \ge 1$. We rewrite (17) to obtain an error bound depending only on h by setting $r = kh^\alpha$:

$$\begin{aligned} |\hat{\kappa}_r(\mathtt{D}_h(X), \hat{x}, h) - \kappa(X, x)| \le\, & O(h^\alpha) + O(h^{\beta - \alpha(1+\beta)}) \\ & + O(h^{\alpha' - 2\alpha}) + O(h^{\alpha'}) + O(h^{2\alpha' - 2\alpha}). \end{aligned} \tag{18}$$

We follow the same idea as for (13) to find the best possible parameter α. The difference is that the optimal α_m depends not only on β but also on α'. Simple computations give $\alpha_m = \frac{\beta}{1+\beta}$ if $\alpha' \ge \frac{3\beta}{1+\beta}$, otherwise $\alpha_m = \frac{\alpha'}{3}$. If point $\hat{x}$ is taken on the digital boundary $\partial_h X$, then $\alpha' = 1$ from the relation $\delta \le \frac{\sqrt{2}}{2}h$ (see above). We obtain then the convergence theorem below.

Theorem 2 (Uniform convergence of curvature estimator $\hat{\kappa}_r$ along $\partial_h X$). *Let X be some convex shape of $\mathbb{R}^2$, with at least C^3-boundary and bounded curvature. Then, $\exists h_0 \in \mathbb{R}^+$, for any $h \le h_0$, setting $r = kh^{\frac{1}{3}}$, we have*

$$\forall x \in \partial X, \forall \hat{x} \in \partial_h X, \|\hat{x} - x\|_\infty \le h \Rightarrow |\hat{\kappa}_r(\mathtt{D}_h(X), \hat{x}, h) - \kappa(X, x)| \le K h^{\frac{1}{3}}.$$

Proof. Let $\hat{x} \in \partial_h X$ and set $x_0 = \pi_h^X(\hat{x})$. We know that $\delta = \|\hat{x} - x_0\|_2 \le \frac{\sqrt{2}}{2}h$. Thus $\alpha' = 1$ and $\alpha_m = \frac{1}{3}$. Then (18) becomes:

$$|\hat{\kappa}_r(\mathtt{D}_h(X), \hat{x}, h) - \kappa(X, x_0)| \le O(h^{\frac{1}{3}}). \tag{19}$$

with $r = kh^{\frac{1}{3}}$, k is an arbitrary positive constant, and $r < r_0$ (constant that depends on X). This implies $h < h_1 \overset{def}{=} (r_0/k)^3$. Let $x \in \partial X$ with $\|\hat{x} - x\|_\infty \le h$. Since $\|\hat{x} - x_0\|_2 \le \frac{\sqrt{2}}{2}h \implies \|\hat{x} - x_0\|_\infty \le \frac{\sqrt{2}}{2}h < h$, we conclude that x and x_0 are under the same closed square Q of edge length $2h$ centered on $\hat{x}$. It is proven that for sufficiently regular shapes (called par(R)-regular shapes in [14], R is the inverse of the maximal curvature) there exists a gridstep $h_2 = \frac{\sqrt{10}}{5}R$ below which the boundary of the shape digitization has same topology as the shape boundary ([12], Theorem B.5). Furthermore, these two boundaries are very close (Hausdorff distance is below h). For $h < R/2 < h_2$, since $Q \cap \partial_h X$ is connected, $Q \cap \partial X$ is connected. Hence x and x_0 both belongs to the same piece of $Q \cap \partial X$, whose length is upper bounded by πh. Since the boundary is C^3 the curvature may only vary between x and x_0 by some $O(\pi h)$. Hence $|\kappa(X, x) - \kappa(X, x_0)| \leq O(h)$. Inserting the previous relation in (19) and observing that $O(h)$ is negligible against $O(h^{\frac{1}{3}})$ allow us to conclude for $h < h_0 \overset{def}{=} \min(h_1, R/2)$. □

Mean and Gaussian curvature in 3D. For the mean curvature, we may follow the same principles as above, using (6) and (7), and inserting the volume estimator $\widehat{\mathrm{Vol}}$ into the formulas. Since (10) holds for $\widehat{\mathrm{Vol}}$ (if γ replaces β), we derive the uniform convergence for the the *integral digital mean curvature estimator* $\hat{H}_r$ of a digital shape $Z' \subset \mathbb{Z}^3$ at point $x \in \mathbb{R}^3$ and step h as:

$$\forall 0 < h < r, \hat{H}_r(Z', x, h) \overset{def}{=} \frac{8}{3r} - \frac{4\widehat{\mathrm{Vol}}(B_{r/h}(\frac{1}{h} \cdot x) \cap Z', h)}{\pi r^4}. \tag{20}$$

If X has C^2-boundary and bounded curvatures, the uniform convergence of $\hat{H}_r$ towards H_r is achieved along ∂X for $r = K' h^{1/3}$, with a speed of convergence of $O(h^{1/3})$. To be valid along $\partial_h X$, it is required to prove that the back-projection has the same properties in 3D as in 2D. This is not developed here for space reasons. Similarly, an integral digital Gaussian curvature estimator can be obtained by digital approximation of the covariance matrices of $X \cap B_r(x)$. Convergence results rely on the fact that digital moments converge in the same manner as volumes [10].

4 Experimental evaluation

We present an experimental evaluation of curvature estimators in 2D and 3D. We have implemented these Integeral Invariant estimators (II) in the `DGtal` library [1] whichallows us to have parametric or implicit shape construction in dimension 2 and 3 for multigrid evaluation. Furthermore, it allows comparison with former approaches available in `DGtal`: Most-centered Digital Circular Arc (MDCA) [19] and Binomial based convolution [5].

As described in Sect. 2, brute-force implementation is trivial. We first need to construct a kernel from an Euclidean ball in dD with radius given by $r = k_m h^{\alpha_m}$ as described in theorem statements. Then, we track the digital object boundary, center the kernel on each surface elements and compute the volume intersection between the kernel and the object. Using this approach, we obtain a computational cost in $O((r/h)^d)$ per surface element (*i.e.* the size of the kernel digitization with grid-step h). However, we can take benefit from digital surface structure to considerably speed-up this algorithm: if we consider a surface tracker for which surface elements are processed by proximity (the current surface element is a neighbor of the previous one through a translation vector $\boldsymbol{\delta}$), the area/volume computation can be done incrementally since they are countable additive:

$$\widehat{\mathrm{Area}}(\mathtt{D}_h(X) \cap B_r(x+\boldsymbol{\delta}), h) = \widehat{\mathrm{Area}}(\mathtt{D}_h(X) \cap B_r(x), h)$$
$$+ \widehat{\mathrm{Area}}(\mathtt{D}_h(X) \cap (B_r(x+\boldsymbol{\delta}) \setminus B_r(x)), h) - \widehat{\mathrm{Area}}(\mathtt{D}_h(X) \cap (B_r(x) \setminus B_r(x+\boldsymbol{\delta})), h).$$

If we precompute all kernels $\mathtt{D}_h(B_r(0 \pm \boldsymbol{\delta}) \setminus B_r(0))$ for some $\boldsymbol{\delta}$ displacements (based on surface element umbrella configurations, 8 in 2D and 26 in 3D for $\|\boldsymbol{\delta}\|_\infty = h$), the computational cost per surface element can be reduced to $O((r/h)^{d-1})$. Finally, the first surfel has to be computed using kernel $B_r(\hat{x})$ and the subsequent neighboring surfels are processed using sub-kernels $\mathtt{D}_h(B_r(0 \pm \boldsymbol{\delta}) \setminus B_r(0))$.

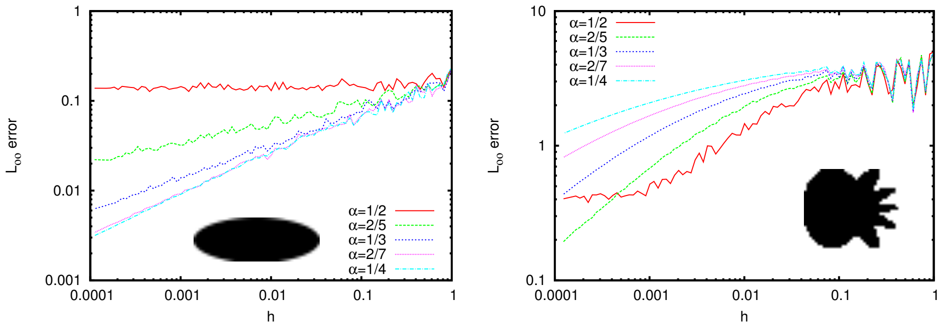

Fig. 2. Comparison of h^α on an ellipse (left) and on the accelerated flower (right).

As discussed in the previous section, we first validate the experimental multigrid convergence for various α_m parameters. Fig. 2 gives results for two 2D shapes: error is given by the l_∞ distance to the true expected values in order to match with theorem settings. For multigrid ellipses (Fig. 2, left) which corresponds to theorem hypothesis (convex C^3 shape), we observe convergence for several α_m values. However, as suggested by Theorem 2, $\alpha_m = \frac{1}{3}$ provides better worst-case errors. Furthermore, note that for $\alpha_m = \frac{1}{3}$, the behavior of the l_∞ error is experimentally in $O(h^{\frac{1}{3}})$ as suggested by the theorem. For non-convex accelerated flower shape (Fig. 2, right), we still observe the convergence but values α_m higher than $\frac{1}{3}$ (and thus larger digital kernel size) seem to lead to lower error values. Further analysis should be done to clearly understand this fact.

In Fig. 3, we compare the proposed 2D curvature estimator (II with $\alpha_m = \frac{1}{3}$) with binomial convolution and MDCA estimator for the l_∞ error metric. In these noise-free object, MDCA performs better than II or Binomial. However, since II and Binomial are based on integration, we may expect better results on noisy objects. Note that in our experiments, observed convergence speeds on ellipses are: $O(h^{0.154})$ for binomial, $O(h^{0.42})$ for MDCA, and $O(h^{0.38})$ for II using least square linear fitting. The first one differs from theoretical results of [5]. In both graphs, we had to stop the computations for Binomial and MDCA for the following reasons: for our implementation of Binomial, the mask size was too large for small h values which induces memory usage issues. For MDCA, circular arc recognition in `DGtal` is driven by a geometrical predicate based on a determinant computation of squared point coordinates. Hence, small h values lead to numerical capacity issues and thus instability (which could be solved considering arbitrary precision integer numbers but would lead to efficiency issues). The proposed integral invariant estimator does not suffer from these two kind of issues. Fig. 4, right, details timings for the 2D accelerated flower and for the 3D blobby cube (see below). We have performed the same analysis in 3D for the mean curvature: evaluation of α_m parameters (Fig. 4, left) on a blobby cube[3]. Concerning the literature and as far as we know, no estimators target multigrid convergence. We have compared with fixed neighborhood convolution as described in [6].

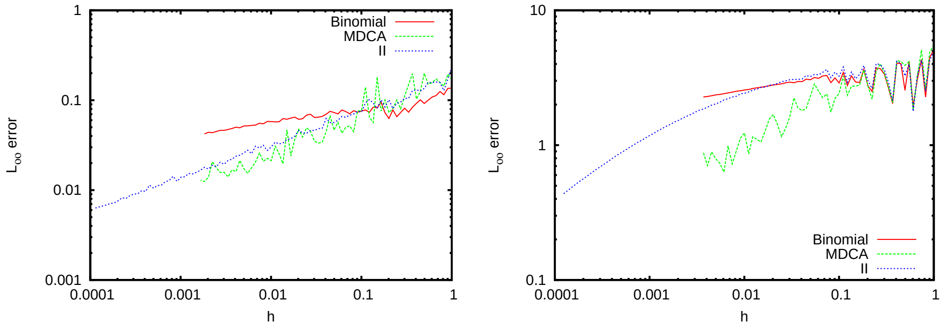

Fig. 3. Comparison of L_∞ error with Binomial [5] and MDCA [19] on multigrid ellipses (left) and accelerated flower (right).

Finally, Fig. 5 illustrates mean and Gaussian curvature estimation in 3D (based on covariance matrix of the intersection between the kernel and the shape) and principal curvature directions (eigenvectors of the covariance matrix). Concerning mean curvature, setting $\alpha_m = \frac{1}{3}$ leads to an experimental convergence speed in $O(h^{0.52})$ for the blobby cube, which means either that $h^{\frac{1}{3}}$ is not a tight upper bound or that tested parameters h are not small enough and far from the asymptotic behavior (note that for the finest experiment $h = 0.0247$, the object surface contains 1277288 elements).

5 Conclusion

In this paper, we have used integral invariant results from differential geometry to design simple and efficient digital curvature estimator in dimension 2 and 3. Digital Geometry is a perfect domain for such differential tools: volume/area

[3] Implicit surface is $81x^4 + 81y^4 + 81z^4 - 45x^2 - 45y^2 - 45z^2 - 6 = 0$.

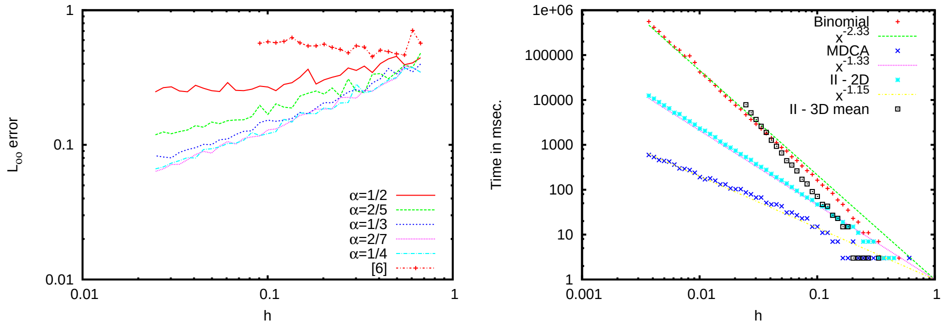

Fig. 4. (Left) Experimental evaluation for mean curvature on blobby cube. (Right) Computational efficiency in dimension 2 (blue, cyan and red) and 3 (black).

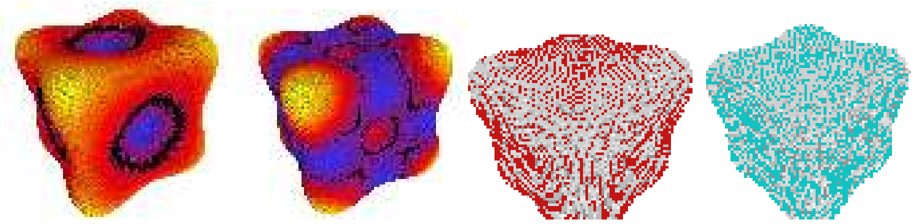

Fig. 5. Illustration of curvature estimation on a 3D blobby cube. *From left to right*: mean curvature and Gaussian curvature mapping ($h = 0.02$, highest is yellow, lowest is blue, red is in-between, furthermore we have set to black zero curvature surfels), first and second principal curvature directions.

computations are digital by nature, interesting connections to fundamental results on Gauss digitization exist, fast computations induced by the specific geometry of digital surfaces. Concerning the 2D curvature estimator, its theoretical convergence speed in $O(h^{\frac{1}{3}})$ on C^3 contours is comparable to state-of-the-art methods ($O(h^{\frac{4}{9}})$ for [5] and $O(h^{\frac{1}{3}})$ for [18]). Evaluation confirms this bound and has demonstrated efficient algorithm in practice with low computational costs. We have also demonstrated that such integral invariants lead to digital mean and Gaussian curvature estimators in 3D. A convergence result for mean curvature has been established and similar results for principal and Gaussian curvatures are expected. Moreover, convergence speed is obtained with a weak constraint on the distance between $\hat{x}$ and x (which just needs to be lower that h for the l_∞ metric). Using specific projection as discussed in [12], better convergence speed is expected at least for dimension 2.

References

1. `DGtal`: Digital geometry tools and algorithms library, http://libdgtal.org

2. Bullard, J.W., Garboczi, E.J., Carter, W.C., Fullet, E.R.: Numerical methods for computing interfacial mean curvature. Computational materials science 4, 103–116 (1995)
3. Coeurjolly, D., Klette, R.: A comparative evaluation of length estimators of digital curves. IEEE Trans. on Pattern Analysis and Machine Intelligence 26(2), 252–258 (2004)
4. Coeurjolly, D., Lachaud, J.O., Roussillon, T.: Digital Geometry Algorithms, Theoretical Foundations and Applications of Computational Imaging, LNCVB, vol. 2, chap. Multigrid convergence of discrete geometric estimators, pp. 395–424. Springer (2012)
5. Esbelin, H.A., Malgouyres, R., Cartade, C.: Convergence of binomial-based derivative estimation for 2 noisy discretized curves. Theoretical Computer Science 412(36), 4805 – 4813 (2011)
6. Fourey, S., Malgouyres, R.: Normals and curvature estimation for digital surfaces based on convolutions. In: Discrete Geometry for Computer Imagery. pp. 287–298 (2008)
7. Guo, J.: On lattice points in large convex bodies. ArXiv e-prints (2010)
8. Huxley, M.N.: Exponential sums and lattice points. Proc. London Math. Soc. 60, 471–502 (1990)
9. Huxley, M.N.: Area, lattice points and exponential sums. Oxford Science publications (1996)
10. Klette, R., Žunić, J.: Multigrid convergence of calculated features in image analysis. Journal of Mathematical Imaging and Vision 13, 173–191 (2000)
11. Krätzel, E.: Lattice points, vol. 33. Springer (1988)
12. Lachaud, J.O.: Espaces non-euclidiens et analyse d'image : modèles déformables riemanniens et discrets, topologie et géométrie discrète. Habilitation à diriger des recherches, Université Bordeaux 1, Talence, France (2006)
13. Lachaud, J.O., de Vieilleville, F.: Convex shapes and convergence speed of discrete tangent estimators. In: Proc. Int. Symposium on Visual Computing. LNCS, vol. 4292, pp. 688–697. Springer (2006)
14. Latecki, L.J., Conrad, C., Gross, A.: Preserving topology by a digitization process. Journal of Mathematical Imaging and Vision 8(2), 131–159 (1998)
15. Malgouyres, R., Brunet, F., Fourey, S.: Binomial convolutions and derivatives estimation from noisy discretizations. In: Discrete Geometry for Computer Imagery. LNCS, vol. 4992, pp. 370–379. Springer (2008)
16. Pottmann, H., Wallner, J., Huang, Q., Yang, Y.: Integral invariants for robust geometry processing. Computer Aided Geometric Design 26(1), 37–60 (2009)
17. Pottmann, H., Wallner, J., Yang, Y., Lai, Y., Hu, S.: Principal curvatures from the integral invariant viewpoint. Computer Aided Geometric Design 24(8-9), 428–442 (2007)
18. Provot, L., Gérard, Y.: Estimation of the derivatives of a digital function with a convergent bounded error. In: Discrete Geometry for Computer Imagery. pp. 284–295 (2011)
19. Roussillon, T., Lachaud, J.O.: Accurate curvature estimation along digital contours with maximal digital circular arcs. In: Combinatorial Image Analysis. vol. 6636, pp. 43–55. Springer (2011)
20. de Vieilleville, F., Lachaud, J.O., Feschet, F.: Maximal digital straight segments and convergence of discrete geometric estimators. Journal of Mathematical Image and Vision 27(2), 471–502 (2007)